

Electronic Supplementary Information

Recorded color rendering index in single Ce,(Pr,Mn):YAG transparent ceramics for high-power white LEDs/LDs

Yuelong Ma ‡^{a, b} Le Zhang ‡^{a, d e *}, Tianyuan Zhou^a, Bingheng Sun^a, Yun Wang^b, Jin Huang^a, Jian Kang^a, Pan Gao^c, Farida A Selim^d, Chingping Wong^e Ming Li^f Hao Chen^{a, *}

^a Jiangsu Key Laboratory of Advanced Laser Materials and Devices, School of Physics and Electronic Engineering, Jiangsu Normal University, Xuzhou, 221116, P.R. China,

^b School of Mechanical Engineering, Jiangsu University, Zhenjiang, 212013, P.R. China

^c College of Materials Science and Engineering, Nanjing Tech University, Nanjing, 210009, PR China

^d Department of Physics and Astronomy, Bowling Green State University, Bowling Green, 43403, USA

^e School of Materials Science and Engineering, Georgia Institute of Technology, Atlanta, 30332, USA

^f Department of Mechanical, Materials and Manufacturing, University of Nottingham, Nottingham NG14BU, UK

* To whom correspondence should be addressed.

Tel: +86-0516-83403242;

E-mail: zhangle@jsnu.edu.cn (Le Zhang), chenhao@jsnu.edu.cn (Hao Chen),

‡ These authors contributed equally to this work.

Table S1. CRI parameter of the reported Ce:YAG TCs

Year	Researchers	Components	CRI	Reference
2016	Hu et al.	YAG:Ce ceramic	73.7	[37]
2017	Tang et al.	Cr/Ce:YAG ceramic	64.6	[19]
2017	Jiang et al.	YAG:Ce,Pr,Cr ceramic	78.0	[20]
2017	Zhang et al.	YAG:Ce ³⁺ -Al ₂ O ₃ eutectic ceramic	75.0	[38]
2018	Shao et al.	(Y,Gd) ₃ Al ₅ O ₁₂ :Ce ceramic	70.7	[39]
2018	Zhang et al.	YAG:Ce ceramic	60.1	[40]
2018	Tang et al.	Ce,Pr:YAG ceramic	62.9	[23]
2019	Zhang et al.	(Cu,Ce):YAG ceramic	68.1	[41]
2019	Wang et al.	YAG:Ce ³⁺ ,Mn ²⁺ ceramic	74.0	[42]
2019	Wang et al.	CaF ₂ -YAG:Ce ceramic	82.7	[15]
2019	Jiang et al.	Gd ₃ Al ₄ GaO ₁₂ :Ce ³⁺ ceramic	78.9	[43]
2019	Li et al.	MgAl ₂ O ₄ -Ce:GdYAG composite ceramic	70.0	[44]
2019	Li et al.	Al ₂ O ₃ -Ce:GdYAG composite ceramic	71.4	[45]
2019	Zhou et al.	(Tb,Gd) ₃ Al ₅ O ₁₂ :Ce ³⁺ ceramic	74.7	[46]

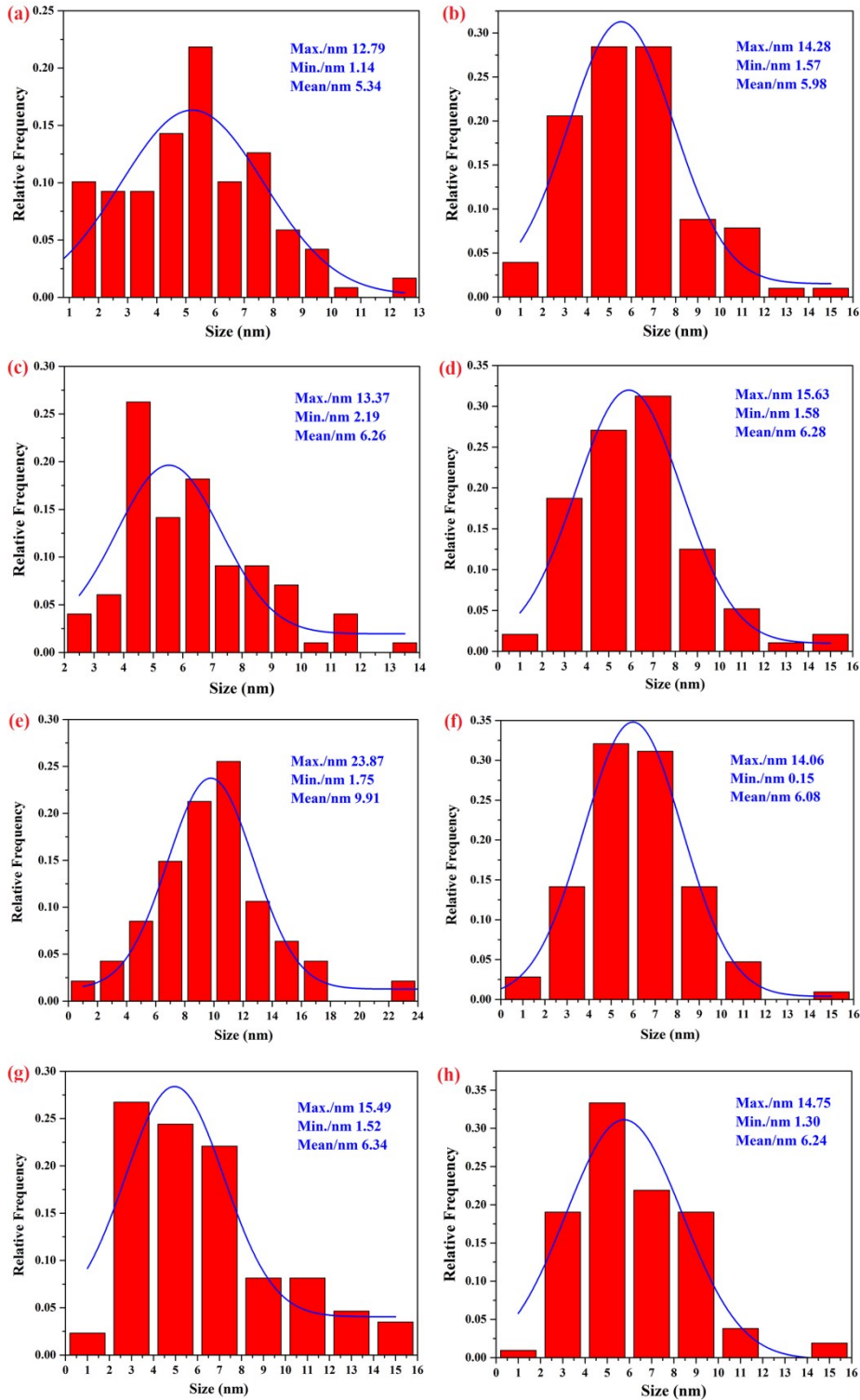


Fig. S1. Particle size distribution of: (a)Pr0Mn0, (b)Pr02Mn0, (c)Pr0Mn04, (d)Pr005Mn05, (e)Pr01Mn06, (f)Pr015Mn07, (g)Pr02Mn08, (h)Pr04Mn10.

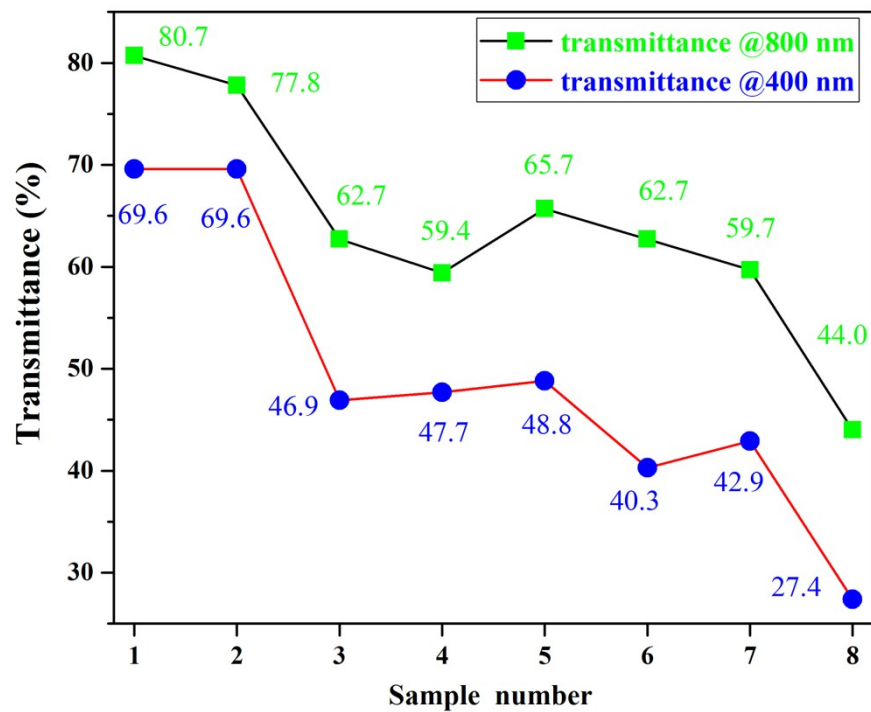


Fig. S2. Optical in-line transmission spectra of the mirror polished samples at 800 nm and 400 nm.

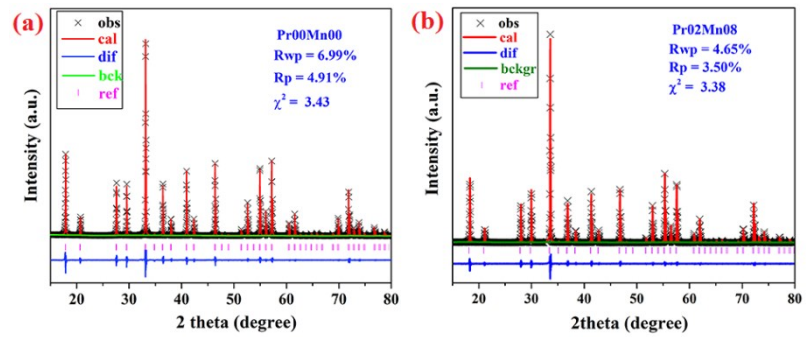


Fig. S3. X-ray Rietveld refinements for Pr00Mn00 and Pr02Mn08 TCs.

Table S2 Main parameters determined with Rietveld refinements of Pr00Mn00 and

Pr02Mn08 TCs.

	Pr00Mn00	Pr02Mn08
Unit cell (Å)	12.006583	12.008131
Cell volume (Å ³)	1730.845	1731.515
Y/Ce1/Pr1-O (Å)	2.3103	2.31470
Y/Ce2/Pr2-O (Å)	2.4406	2.45753
Al/Mn-O(1) (Å)	1.77078	1.76286
Al/Mn-O(2) (Å)	1.98356	2.00034
Polyhedron distortion ratio D	0.02743	0.02992
Reliability factors		
Rwp	6.99%	4.65%
Rp	4.91%	3.50%
χ^2	3.43	3.38

Polyhedron distortion ratio D can be quantitatively calculated using the following Eq. (1):

$$D = \frac{1}{n} \sum ((L_i - L_{av}) / L_{av})$$

where L_i is the distance from the cation to “ i ” coordinated oxygen atom, and L_{av} is the average bond length.

Table S3. The color coordinates, CRI, CCT and LER of the fabricated TC-based white LDs.

Samples	CRI	Color coordinates (x, y)		CCT (K)	LER (lm/W)
		x	y		
Pr0Mn0	51.1	0.4175	0.4871	3894	131.9
Pr02Mn0	55.2	0.4225	0.4631	3880	101.7
Pr0Mn04	58.8	0.4281	0.4865	3666	68.4
Pr005Mn05	56.9	0.4207	0.4050	3702	82.9
Pr01Mn06	63.8	0.4264	0.4382	3440	50.4
Pr015Mn07	68.3	0.4207	0.4050	3299	32.8
Pr02Mn08	70.5	0.4017	0.3869	3550	28.7
Pr04Mn10	62.2	0.4155	0.4344	3613	47.1

Formula S1;

The luminous efficiency of radiation (LER) was calculated by the following equation:

$$LER = \frac{\Phi}{P} = \frac{K_m \int V(\lambda)S(\lambda)}{\int S(\lambda)d\lambda}$$

Where Φ is luminous flux, P is the power of input, K_m is the maximum luminous efficacy of radiation (approximately 683 lm/W). $S(\lambda)$ is the spectral distribution of the light source and $V(\lambda)$ is the 1924 CIE relative luminous efficiency function of photopic vision that is defined in the vision range of 380-780 nm.

Table S4. The CCT of the fabricated TC-based WLED under different working current.

Current(mA)	Pr0Mn0(K)	Pr02Mn0(K)	Pr0Mn04(K)	Pr005Mn05(K)	Pr01Mn06(K)	Pr015Mn07(K)	Pr02Mn08(K)	Pr04Mn10(K)
100	4336	4922	4509	4285	4499	4577	4895	4217
150	4349	4900	4647	4292	4642	4600	4981	4270
200	4366	4922	4595	4336	4688	4570	4935	4176
250	4407	5162	4610	4312	4691	4745	4954	4236
300	4292	4850	4629	4263	4799	4664	5227	4261
350	4272	4796	4550	4188	4698	4829	5460	4173
400	4434	4979	4725	4288	4688	4658	5062	4333

Table S5. The CRI of the fabricated TC-based WLED under different LED working current.

Current (mA)	Pr0Mn0	Pr02Mn0	Pr0Mn04	Pr005Mn05	Pr01Mn06	Pr015Mn07	Pr02Mn08	Pr04Mn10
100	56.7	67.2	70.3	65.7	77.6	80.6	82.7	72.1
150	56.6	66.8	70.9	65.5	77.7	81.2	83.1	72.3
200	56.6	66.8	70.5	65.7	77.4	81.3	83.4	71.2
250	57.1	68.6	70.1	65.4	78.0	81.6	83.5	71.7
300	56.1	66.4	70.6	65.1	77.6	81.7	84.2	71.9
350	56.6	67.6	70.7	65.7	79.4	83.3	84.8	72.5
400	56.7	66.7	70.4	64.7	77.1	81.1	83.6	71.9

Table S6. The color coordinates of the fabricated TC-based WLED under different LED working current (Pr0Mn0-Pr005Mn05).

Current (mA)	Pr0Mn0		Pr02Mn0		Pr0Mn04		Pr005Mn05	
	x	y	x	y	x	y	x	y
100	0.3830	0.4464	0.3508	0.3875	0.3629	0.3771	0.3785	0.4144
150	0.3817	0.4431	0.3514	0.3857	0.3569	0.3675	0.3776	0.4119
200	0.3814	0.4450	0.3503	0.3830	0.3585	0.3671	0.3748	0.4068
250	0.3768	0.4318	0.3418	0.3643	0.3583	0.3691	0.3760	0.4078
300	0.3846	0.4442	0.3526	0.3823	0.3565	0.3613	0.3780	0.4078
350	0.3837	0.4358	0.3528	0.3700	0.3591	0.3626	0.3791	0.3999
400	0.3769	0.4381	0.3480	0.3769	0.3538	0.3620	0.3776	0.4111

Table S7. The color coordinates of the fabricated TC-based WLED with different LED working current (Pr01Mn06-Pr04Mn10).

Current (mA)	Pr01Mn06		Pr015Mn07		Pr02Mn08		Pr04Mn10	
	x	y	x	y	x	y	x	y
100	0.3571	0.3551	0.3566	0.3400	0.3447	0.3229	0.3734	0.3802
150	0.3558	0.3513	0.3518	0.3324	0.3425	0.3180	0.3703	0.3742
200	0.3566	0.3515	0.3505	0.3308	0.3425	0.3185	0.3750	0.3806
250	0.3508	0.3438	0.3500	0.3281	0.3430	0.3176	0.3713	0.3735
300	0.3533	0.3459	0.3471	0.3248	0.3370	0.3084	0.3698	0.3707
350	0.3509	0.3353	0.3453	0.3153	0.3327	0.2951	0.3710	0.3632
400	0.3535	0.3467	0.3502	0.3292	0.3405	0.3135	0.3669	0.3684